

# Effective Majorana neutrino decay

Lucía Duarte<sup>1,a</sup>, Ismael Romero<sup>2</sup>, Javier Peressutti<sup>2</sup>, Oscar A. Sampayo<sup>2,b</sup>

<sup>1</sup> Instituto de Física, Facultad de Ingeniería, Universidad de la República, Julio Herrera y Reissig 565, 11300 Montevideo, Uruguay

<sup>2</sup> Departamento de Física, Instituto de Investigaciones Físicas de Mar del Plata (IFIMAR) CONICET, UNMDP, Universidad Nacional de Mar del Plata, Funes 3350, 7600 Mar del Plata, Argentina

Received: 24 April 2016 / Accepted: 1 August 2016 / Published online: 11 August 2016  
© The Author(s) 2016. This article is published with open access at Springerlink.com

**Abstract** We study the decay of heavy sterile Majorana neutrinos according to the interactions obtained from an effective general theory. We describe the two- and three-body decays for a wide range of neutrino masses. The results obtained and presented in this work could be useful for the study of the production and detection of these particles in a variety of high energy physics experiments and astrophysical observations. We show in different figures the dominant branching ratios and the total decay width.

## 1 Introduction

The discovery of neutrino oscillations has been one of the most spectacular new results in high energy physics, and so far is the only compelling experimental evidence of the existence of physics beyond the Standard Model. The sub-eV left-handed neutrino masses required by neutrino oscillation data are very difficult to generate just by the addition of right-handed neutrinos to the Standard Model, as the Yukawa couplings should be very small compared to those of the other particles. The introduction of intermediate fermion heavy particles which are singlets under the  $SM$  gauge group—the right-handed Majorana neutrinos—allows for the generation of light neutrino masses by the seesaw mechanism [1–6].

For the conventional seesaw scenarios often studied, the light neutrino masses are inversely proportional to an unknown lepton number violating large scale  $M_N$  such that  $m_\nu \sim m_D^2/M_N$  where  $m_D$  is a Dirac mass connected with the Yukawa coupling by  $m_D = Yv/\sqrt{2}$ , being  $v$  the Higgs field vacuum expectation value. For Yukawa couplings of order  $Y \sim 1$  we need a Majorana mass scale of order  $M_N \sim 10^{15}$  GeV to account for a light  $\nu$  mass compatible with the current neutrino data ( $m_\nu \sim 0.01$  eV). This

scenario clearly leads to the decoupling of the heavy Majorana neutrino  $N$ . However, for smaller Yukawa couplings of the order  $Y \sim 10^{-8} - 10^{-6}$ , sterile neutrinos with masses  $M_N \sim (1 - 1000)$  GeV could exist. Any way, in the simplest Type-I seesaw scenario with sterile neutrinos, this leads to a too small left-right neutrino mixing [7–9],  $U_{iN}^2 \sim m_\nu/M_N \sim 10^{-14} - 10^{-10}$ . These values are several orders of magnitude smaller than the neutrinoless double beta decay ( $0\nu\beta\beta$ ) or collider bounds, as will be shown later.

Thus, as it was explained in [9], the detection of Majorana neutrinos would be a signal of physics beyond the minimal seesaw mechanism leading to the well known  $\nu SM$  lagrangian, and its interactions could be better described in a model-independent approach based on an effective theory, considering a scenario with only one Majorana neutrino  $N$  and negligible mixing with the  $\nu_L$ .

The possibilities of discovering heavy Majorana neutrinos have been and are still extensively investigated, for example involving production and decay in  $e^+e^-$  and  $e^-P$  colliders [10–17], in  $e^- \gamma$  and  $\gamma\gamma$  colliders [18–20], in hadron colliders via lepton number violating dilepton signals [9, 21–30], and recently including new production mechanisms [31–33]. Some searches are currently being performed in the LHC [34–37]. Also, we can mention recent inverse seesaw mechanism (ISS) [38–40] heavy neutrino production studies in collider contexts [41–44].

The study of sterile Majorana neutrino decays is an issue of great interest in different areas of high energy physics. Besides the mentioned detection in colliders by lepton number violation, other kinds of searches exploiting the displaced vertex and delayed photons techniques have been proposed and are taking place at the LHC [45–52]. Also, searches in neutrino telescopes like Ice Cube [53, 54] have been proposed, and the new decay modes and their relation with the explanation of several anomalies as the sub-horizontal events detected by SHALON or the anomaly in MiniBoone [55, 56] are being investigated [57, 58]. In astrophysical envi-

<sup>a</sup> e-mail: [lduarte@fing.edu.uy](mailto:lduarte@fing.edu.uy)

<sup>b</sup> e-mail: [sampayo@mdp.edu.ar](mailto:sampayo@mdp.edu.ar)

ronments, the cosmic and the diffuse supernova neutrino backgrounds can be used to probe possible radiative decays and other decay modes of cosmological interest [59,60].

With these motivations in mind, in this work we study the decays of heavy Majorana neutrinos in a general, model-independent approach in the context of an effective theory. In Sect. 2 we present the effective operators and the analytical decay widths obtained for the different two-body and three-body channels. In Sect. 3 we present our numerical results for the found decay modes, and discuss the bounds imposed on the values for the effective couplings. Our final remarks are made in Sect. 4. The complete effective lagrangian and fermionic decay modes are left for the appendix.

## 2 Effective operators and decay widths

In this paper we consider the decays of a right-handed Majorana neutrino  $N$ . As it is a  $SM$  singlet, the only possible renormalizable interactions with the  $SM$  fields could occur via the Yukawa coupling, which as we mentioned earlier, must be very small if the  $\nu SM$  is to reproduce the observed tiny  $\nu_L$  masses. In an alternative approach, in this paper we consider that the sterile  $N$  interacts with the standard light neutrinos by effective operators of higher dimension. We consider this effective interaction to be dominant compared to the mixing via the Yukawa couplings, so we depart from the traditional viewpoint in which the sterile neutrinos mixing with the standard neutrinos is assumed to govern the production and decay mechanisms for the  $N$ .

In this approach we parameterize the effects of new physics beyond the standard model by a set of effective operators  $\mathcal{O}$  constructed with the standard model and the Majorana neutrino fields and satisfying the Standard Model  $SU(2)_L \otimes U(1)_Y$  gauge symmetry [61]. The effect of these operators is suppressed by inverse powers of the new physics scale  $\Lambda$ -which is not necessarily related to the mass  $m_N$ -for which we take the value  $\Lambda = 1$  TeV [62].

The total lagrangian is organized as follows:

$$\mathcal{L} = \mathcal{L}_{SM} + \sum_{n=6}^{\infty} \frac{1}{\Lambda^{n-4}} \sum_i \alpha_i \mathcal{O}_i^{(n)}. \tag{1}$$

For the considered operators we follow [9] starting with a rather general effective lagrangian density for the interaction of right-handed Majorana neutrinos  $N$  with leptons and quarks. All the operators we list here are of dimension 6 and could be generated at tree-level in the unknown fundamental high energy theory. The first subset includes operators with scalar and vector bosons (SVB),

$$\begin{aligned} \mathcal{O}_{LN\phi} &= (\phi^\dagger \phi)(\bar{L}_i N \tilde{\phi}), \quad \mathcal{O}_{NN\phi} = i(\phi^\dagger D_\mu \phi)(\bar{N} \gamma^\mu N), \\ \mathcal{O}_{Ne\phi} &= i(\phi^T \epsilon D_\mu \phi)(\bar{N} \gamma^\mu e_i) \end{aligned} \tag{2}$$

and a second subset includes the baryon-number conserving four-fermion contact terms:

$$\begin{aligned} \mathcal{O}_{duNe} &= (\bar{d}_i \gamma^\mu u_i)(\bar{N} \gamma_\mu e_i), \quad \mathcal{O}_{fNN} = (\bar{f}_i \gamma^\mu f_i)(\bar{N} \gamma_\mu N), \\ \mathcal{O}_{LNL e} &= (\bar{L}_i N) \epsilon (\bar{L}_i e_i), \quad \mathcal{O}_{LNQd} = (\bar{L}_i N) \epsilon (\bar{Q}_i d_i), \\ \mathcal{O}_{QuNL} &= (\bar{Q}_i u_i)(\bar{N} L_i), \quad \mathcal{O}_{QN Ld} = (\bar{Q}_i N) \epsilon (\bar{L}_i d_i), \\ \mathcal{O}_{LN} &= |\bar{N} L_i|^2, \end{aligned} \tag{3}$$

where  $e_i, u_i, d_i$  and  $L_i, Q_i$  denote, for the family labeled  $i$ , the right-handed  $SU(2)$  singlet and the left-handed  $SU(2)$  doublets, respectively.

In addition, there are operators generated at one-loop level in the underlying full theory whose coefficients are naturally suppressed by a factor  $1/16\pi^2$  [9,63]:

$$\begin{aligned} \mathcal{O}_{NNB}^{(5)} &= \bar{N} \sigma^{\mu\nu} N^c B_{\mu\nu}, \\ \mathcal{O}_{NB} &= (\bar{L} \sigma^{\mu\nu} N) \tilde{\phi} B_{\mu\nu}, \quad \mathcal{O}_{NW} = (\bar{L} \sigma^{\mu\nu} \tau^I N) \tilde{\phi} W_{\mu\nu}^I, \\ \mathcal{O}_{DN} &= (\bar{L} D_\mu N) D^\mu \tilde{\phi}, \quad \mathcal{O}_{\bar{D}N} = (D_\mu \bar{L} N) D^\mu \tilde{\phi}. \end{aligned} \tag{4}$$

### 2.1 Two-body decays

The two-body decay channels for the heavy Majorana neutrino  $N$  are shown in Fig. 1. They receive contributions from the lagrangian terms originating with operators involving gauge bosons and the Higgs field, presented in (2) and (4), that lead to the effective lagrangian presented in (A1) and (A3).

The analytical expressions obtained for the decay widths of channels  $N \rightarrow \nu Z, N \rightarrow l^+ W^-, N \rightarrow \nu h$  shown in Fig. 1 are

$$\begin{aligned} \Gamma^{N \rightarrow \nu_i Z} &= \left(\frac{m_N}{128\pi}\right) \left(\frac{m_N}{\Lambda}\right)^4 (1-y_Z)^2 \left[ (\alpha_{L_4}^{(i)} - \alpha_{L_2}^{(i)})^2 (1-y_Z)^2 \right. \\ &\quad + 8(\alpha_{L_4}^{(i)} - \alpha_{L_2}^{(i)}) (\alpha_{L_3}^{(i)} c_W - \alpha_{L_1}^{(i)} s_W) (1-y_Z) \sqrt{y_Z y_\nu} \\ &\quad \left. + 16(2+y_Z) y_\nu (\alpha_{L_3}^{(i)} c_W - \alpha_{L_1}^{(i)} s_W)^2 \right] \end{aligned}$$

with  $y_Z = m_Z^2/m_N^2$  and  $y_\nu = v^2/m_N^2$ ;

$$\Gamma^{N \rightarrow l_i W} = \frac{m_N}{32\pi} \left(\frac{m_N}{\Lambda}\right)^4 \alpha_W^{(i)} (1-y_W)^2 (1+2y_W) y_\nu$$

with  $y_W = m_W^2/m_N^2$ .

$$\Gamma^{(N \rightarrow \nu_i h)} = \frac{9m_N}{128\pi} \left(\frac{v}{\Lambda}\right)^4 \alpha_\phi^{(i)2} (1-y_h)$$

with  $y_h = m_h^2/m_N^2$ .

Finally, we have the decay mode to a photon and an ordinary neutrino,  $N \rightarrow \nu A$ :

$$\Gamma^{N \rightarrow \nu_i A} = \frac{1}{4\pi} \left(\frac{v^2}{m_N}\right) \left(\frac{m_N}{\Lambda}\right)^4 (\alpha_{L_1}^{(i)} c_W + \alpha_{L_3}^{(i)} s_W)^2. \tag{5}$$

This decay mode leads to an interesting phenomenology, part of which was discussed in [58].

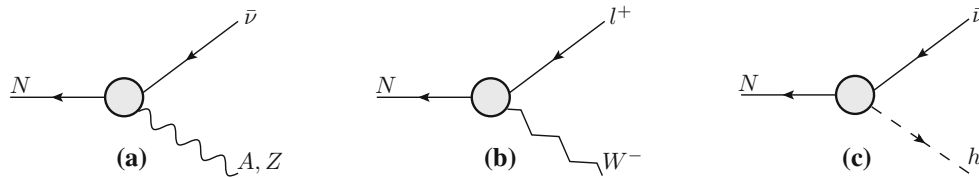


Fig. 1 Two-body decays with gauge bosons and Higgs field

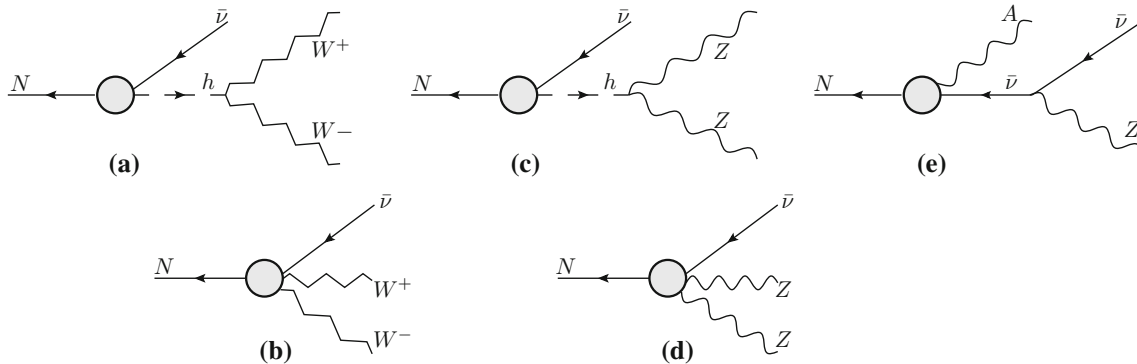


Fig. 2 Three-body decays with two gauge bosons and ordinary neutrinos

It is important to take into account here that the  $W$  and  $h$  resonant contributions to other decays, as can be seen in Fig. 5(a), (b) were already included in those decays and will not be added to the total width.

2.2 Three-body decays

The three-body decays of the heavy Majorana neutrino  $N$  involving gauge bosons and the Higgs field receive contributions from the lagrangians presented in (A1) and (A3), whereas the decays to three fermions come also from the operators presented in (3). The effective model we are working with also gives tree-level contributions to four-body decays, but as their contributions are very small, they are not presented in this work.

The three-body decay channels involving gauge bosons and ordinary neutrinos are shown in Fig. 2; (a) and (b)  $N \rightarrow \nu W^+ W^-$ , (c) and (d)  $N \rightarrow \nu ZZ$ , and (e)  $N \rightarrow \nu ZA$ .

The analytical expressions for the decay widths are

$$\frac{d\Gamma^{N \rightarrow \nu_i W^+ W^-}}{dx} = \frac{m_N}{6144\pi^3} \left(\frac{m_N}{\Lambda}\right)^4 \frac{x^2}{(1-x)^2 y_W} \times ((1-x)(1-x-4y_W))^{1/2} \times \left[ 16\alpha_{L_3}^{(i)2} (3-x)((1-x)^2 + 4(1-x)y_W - 8y_W^2) + 3|\tilde{\alpha}^{(i)}|^2 g^2(1-x)((1-x)^2 - 4(1-x)y_W + 12y_W^2) \right]$$

where  $\tilde{\alpha}^{(i)} = \alpha_{L_4}^{(i)} + \frac{3}{2}\alpha_\phi^{(i)} \frac{y_\nu}{1-x-y_h+i\sqrt{y_h y_{\Gamma_h}}}$ ,  $y_{\Gamma_h} = \Gamma_h^2/m_N^2$ . In this process we discard the  $N \rightarrow lW$  followed by the  $l \rightarrow \nu W$  SM vertex contribution, because the amplitude is proportional to the intermediate lepton mass, and thus negligible in comparison with the diagrams shown in Fig. 2(a), (b).

$$\frac{d\Gamma^{N \rightarrow \nu_i ZZ}}{dx} = \frac{m_N}{64\pi^2} \left(\frac{m_N}{\Lambda}\right)^4 \frac{\alpha^{emg}}{s_{2W}^2} y_Z \times \left[ \left( \alpha_{L_4}^{(i)} + \frac{3\alpha_\phi^{(i)} y_\nu (1-x-y_h)}{(1-x-y_h)^2 + y_h y_{\Gamma_h}} \right)^2 + \left( \frac{3\alpha_\phi^{(i)} y_\nu \sqrt{y_h y_\nu}}{(1-x-y_h)^2 + y_h y_{\Gamma_h}} \right)^2 \right] \times \frac{x^2}{(1-x)} \left( 2 + \frac{(1-x-2y_Z)^2}{4y_Z^2} \right) \times ((1-x-2y_Z)^2 - 4y_Z^2)^{1/2}$$

with  $\alpha^{emg}$  being the electromagnetic constant, and  $y_{\Gamma_h} = \Gamma_h^2/m_N^2$ .

$$\frac{d\Gamma^{N \rightarrow \nu_i ZA}}{dx} = \frac{m_N}{32\pi^3} \left(\frac{m_N}{\Lambda}\right)^4 (c_W \alpha_{L_1}^{(i)} + s_W \alpha_{L_3}^{(i)})^2 \times \frac{(1-x+2y_Z)(1-x-y_Z)x^3}{(1-x)^3}$$

The three-body channels with Higgs fields in the final state are shown in Fig. 3 (a)  $N \rightarrow \nu hh$ , (b)  $N \rightarrow l^+ W^- h$ , (c)  $N \rightarrow \nu h A$ , and (d)  $N \rightarrow \nu h Z$ . The obtained expressions for the decay widths are

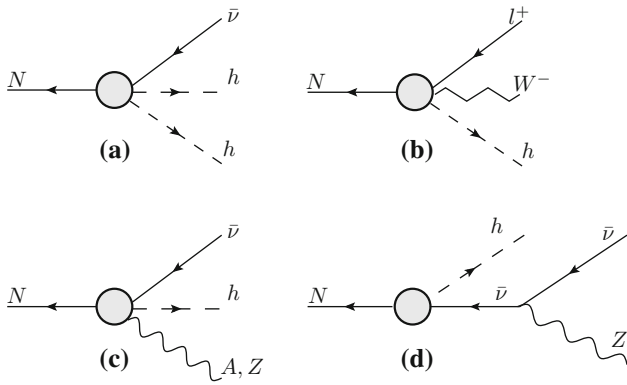


**Fig. 3** Three-body decays with gauge bosons and Higgs field

$$\frac{d\Gamma^{N \rightarrow \nu_i hh}}{dx} = \frac{18\alpha_W^{(i)2} m_N}{2048\pi^3} \left(\frac{v}{m_N}\right)^2 \left(\frac{m_N}{\Lambda}\right)^4 x^2 \times \frac{((1-x-2y_h)^2 - 4y_h^2)^{1/2}}{(1-x)}$$

with  $0 \leq x \leq 1 - 4y_h$ ;

$$\frac{d\Gamma^{N \rightarrow l_i Wh}}{dx} = \frac{m_N \alpha_W^{(i)2}}{768\pi^3} \left(\frac{m_N}{\Lambda}\right)^4 ((1-x-y_h)^2 - 2(1-x+y_h)y_W + 4y_W^2)^{1/2} \times \left[ (3-x) \left( (1-x-y_h)^2 + y_W^2 \right) + (6-3y_h + x(-11+5x+y_h))y_W \right] \frac{x^2}{(1-x)^3},$$

$$\frac{d\Gamma^{N \rightarrow \nu_i Ah}}{dx} = \frac{m_N}{192\pi^3} \left(\frac{m_N}{\Lambda}\right)^4 (c_W \alpha_{L_1}^{(i)} + s_W \alpha_{L_3}^{(i)})^2 \frac{(1-x-y_h)^3 x^3}{(1-x)^3}$$

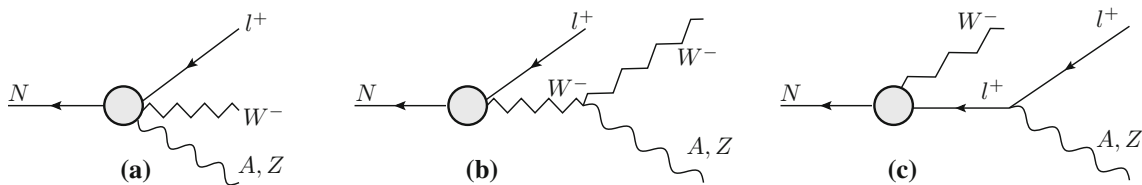


**Fig. 4** Three-body decays with two gauge bosons and charged leptons

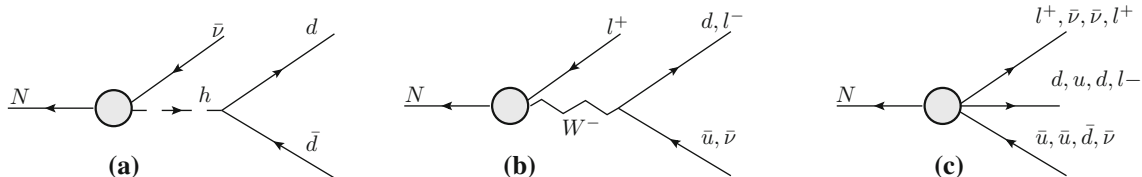


**Fig. 5** Majorana neutrino decaying to three fermions

with  $0 \leq x \leq 1 - y_h$ ;

$$\frac{d\Gamma^{N \rightarrow \nu_i Zh}}{dx} = \frac{9 m_N g^2}{2^{14} \pi^3} \left(\frac{v}{\Lambda}\right)^4 \alpha_\phi^{(i)2} \times \left[ \frac{(2-x)(1-x+y_h+2y_z)(1-x+y_h-y_z)(x^2 - 4y_h)^{1/2}}{y_z(1-x+y_h)} \right]$$

with  $2\sqrt{y_h} \leq x \leq 1 + y_h - y_z$ . This decay width is obtained from the diagram shown in Fig. 3(d), as this contribution involves a tree-level vertex coming from the lagrangian (A1) and a SM vertex, and is dominant comparing to the one-loop level term coming from the lagrangian (A3), that would give a vertex as the one shown in Fig. 3(c).

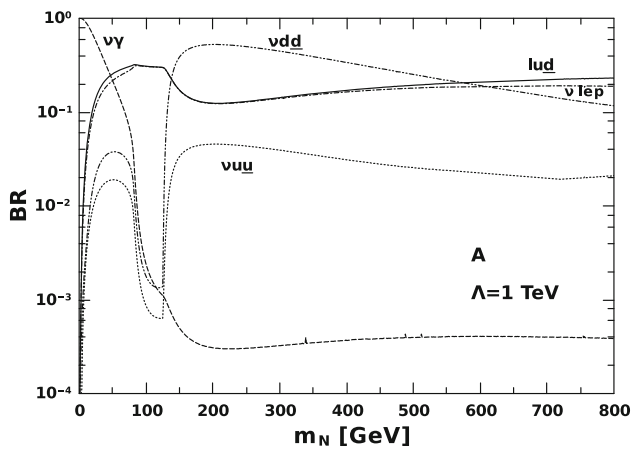
The three-body decay channels with two gauge bosons and charged leptons in the final state are shown in Fig. 4, where  $N \rightarrow l^+ W^- A, Z$ . We cannot obtain analytical expressions for these decay widths, and we have done numerical integrations of the phase space in the usual way using the numerical routine RAMBO [64].

Some of the three-body decays involving only fermions in the final state come from the four-fermion contact operators presented in (3). These operators lead to the tree-level lagrangian in (A2).

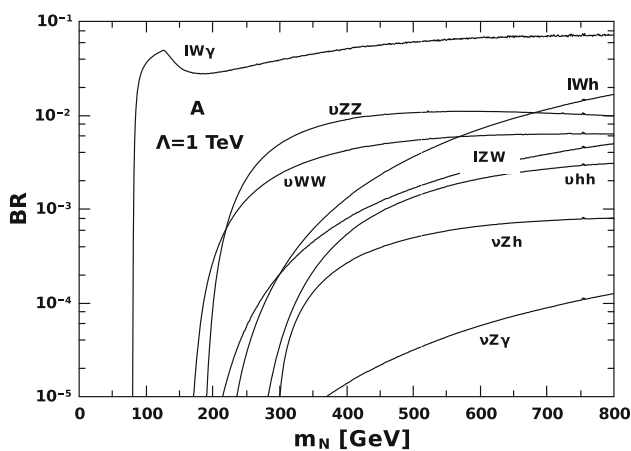
The partial decay widths of a heavy Majorana neutrino  $N$  decaying to three fermions were calculated including the contributions in the effective lagrangians (A1) and (A2). The decay channels are shown in Fig. 5. As was previously mentioned, the diagrams (a) and (b) show the resonant contributions coming from two-body decays to  $W$  and  $h$  bosons. The analytical expressions obtained were presented in our previous work [58], and for completeness we display them in Appendix B.

### 3 Numerical branching ratios and total decay width

The numerical results for the Majorana neutrino branching ratios and total decay width are presented in the following. In Figs. 6 and 7 we show the results for the branching ratios for the different decay channels found in the previous section. We display the branching ratios as a function of the Majorana neutrino mass  $m_N$ , calculated for different numerical values of the constants  $\alpha^i_{\mathcal{O}}$ . In all the following results, when ordinary neutrinos are present in the final states, we sum the contributions of the neutrino and antineutrino channels. It is important to realize that, as we explained in the introduction, we are neglecting the contributions of the  $N-\nu_L$  mixings compared to the effective interactions. In this condition the effective contribution to the branching ratios that we present here are dominant for the scale  $\Lambda = 1$  TeV considered and for the values of  $\alpha$  allowed by experimental data, as will be explained in the next section.



(a) Three fermions and neutrino-photon decay channels.



(b) Massive gauge and Higgs boson decay channels

**Fig. 6** The Branching ratios for the Majorana neutrino decay in the set A considering the sum of families

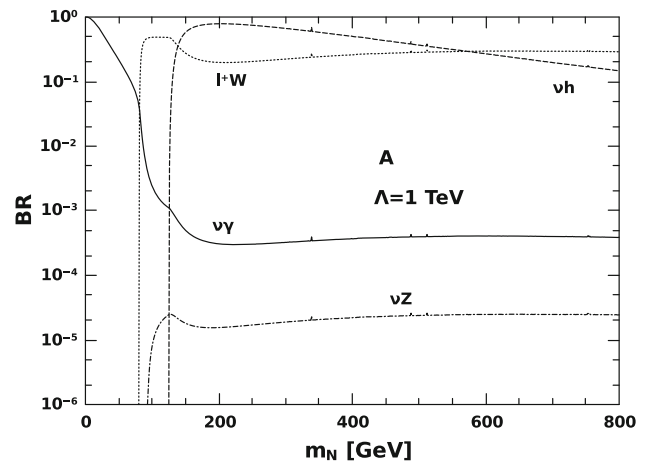


**Fig. 7** The branching ratios for two-body decays considering the sum over families

The values for the coupling constants  $\alpha$  are limited by bounds coming from electroweak precision data (EWPD) and  $0\nu\beta\beta$ -decay data. In order to simplify the discussion we consider just two numerical sets of values: in set **A** the couplings associated to the operators that contribute to the  $0\nu\beta\beta$ -decay are restricted to the corresponding bound,  $\alpha_{0\nu\beta\beta}^{\text{bound}}$  (8) and the other constants are restricted to the bound determined by EWPD  $\alpha_{\text{EWPD}}^{\text{bound}}$  (9) (see next section). In the case of the set **B** all the couplings are restricted to the  $0\nu\beta\beta$  bound  $\alpha_{0\nu\beta\beta}^{\text{bound}}$ , which is the most stringent. The branching ratios, being quotients between partial widths, take very similar numerical values for the two sets.

In Fig. 6a we present the branching ratios of the three-fermion and photon–neutrino channels for the couplings set **A**. These are the only open channels for Majorana neutrino masses below  $m_W$ . As it can be seen, for low  $m_N$  the dominant mode is the decay of  $N$  to a photon and a neutrino. Taking the values of the couplings  $\alpha^{(i)}$  to be equal for every family  $i$ , and also for every tree-level coupling  $\alpha^{\text{tree}}$ , and taking the one-loop generated couplings as  $\alpha^{1\text{-loop}} = \alpha^{\text{tree}}/16\pi^2$ , we derived an approximated expression for the ratio between the widths  $\Gamma(N \rightarrow \nu(\bar{\nu})A)$  in (5) and  $\Gamma(N \rightarrow l^+\bar{u}d)$  in (B1):

$$\frac{\Gamma(N \rightarrow \nu(\bar{\nu})A)}{\Gamma(N \rightarrow l^+\bar{u}d)} \rightarrow \frac{2}{15\pi} \left(\frac{v}{m_N}\right)^2 (c_W + s_W)^2.$$

This limiting value explains the behavior found in Fig. 6a, showing the neutrino plus photon decay channel is clearly dominating for low  $m_N$  (in [58] we verify that this channel still dominates over the decay of  $N$  to QCD-mesons like pions). This is an interesting fact since we have a new source of photons in astrophysical environments. The implications of this new channel for the MiniBoone [65] and SHALON [66] anomalies were discussed in our previous work [58].



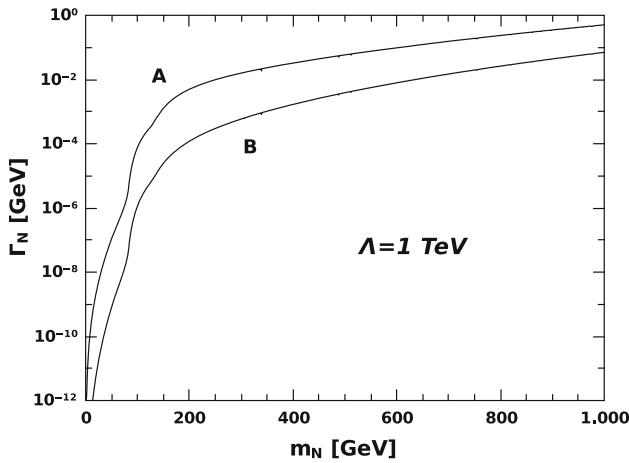


**Fig. 8** Total decay width with coupling constants in the set **A** (solid line) and set **B** (dashed line), and  $\Lambda = 1 \text{ TeV}$

Figure 6(b) shows the massive gauge and Higgs boson decay channels for the  $N$ . The branching ratio for the  $N \rightarrow \nu h A$  mode is smaller than  $1 \times 10^{-7}$  and is not visible in the plot.

For completeness we present the branching ratios for the two-body decay channels. As we explained in the previous section, the  $N \rightarrow \nu h, W$  channels are not included in the total width, as their contribution has already been taken into account in the channels where the  $W$  and  $h$  bosons participate as intermediate resonant states.

Finally, Fig. 8 shows the total decay width dependence on the mass  $m_N$  for both coupling sets considered, and again a sum over families and channels with particles and antiparticles in the final state is performed.

### 3.1 Bounds on the couplings $\alpha_{\mathcal{O}}^i$

The effective couplings  $\alpha_{\mathcal{O}}^i$  can be bounded exploiting the existing constraints coming from neutrinoless double beta decay ( $0\nu\beta\beta$ ), electroweak precision data tests (EWPD), low energy observables as rare lepton number violating (LNV) meson decays and direct collider searches, including  $Z$  decays. We explain here in detail how we take account of the existing bounds for the sterile-active neutrino mixings and turn them into constraints on the effective couplings  $\alpha_{\mathcal{O}}^i$ . In the literature, the bounds are generally imposed on the parameters representing the mixing between the sterile and active left-handed ordinary neutrinos. Very recent reviews [7,8,16,67] summarize in general phenomenological approaches the existing experimental bounds, considering low scale minimal seesaw models, parameterized by a single heavy neutrino mass scale  $M_N$  and a light-heavy mixing  $U_{lN}$ , with  $l$  indicating the lepton flavor. In the effective lagrangian framework we are studying, the heavy Majorana neutrino couples to the three fermion family flavors with cou-

plings dependent on the new ultraviolet physics scale  $\Lambda$  and the constants  $\alpha_{\mathcal{O}}^{(i)}$ . We can interpret the current bounds comparing our couplings with the general structure usually taken for the interaction between heavy neutrinos with the standard gauge bosons [68,69]:

$$\begin{aligned} \mathcal{L}_W &= -\frac{g}{\sqrt{2}} \bar{l} \gamma^\mu U_{lN} P_L N W_\mu + h.c. \\ \mathcal{L}_Z &= -\frac{g}{2c_W} \bar{\nu}_L \gamma^\mu U_{lN} P_L N Z_\mu + h.c. \end{aligned} \tag{6}$$

The operators presented in (2) lead to a term in the effective lagrangian (A1) that can be compared to the interaction in (6) for the weak charged current, giving a relation between the coupling  $\alpha_W^{(i)}$  and the mixing  $U_{lN}$ :  $U_{li} N \simeq \frac{\alpha_W^{(i)} v^2}{2\Lambda^2}$  [9]. Nevertheless, as we are neglecting the  $N-\nu_L$  neutrino mixing, no operators lead to a term that can be directly related—with the same Lorentz-Dirac structure—to the interaction in (6) for the neutral current (nor at tree or one-loop level). Some terms in the lagrangian (A3) contribute to the  $ZN\nu$  coupling, but as they are generated at one-loop level in the ultraviolet underlying theory, they are suppressed by a  $1/16\pi^2$  factor. In consequence, we take a conservative approach and in order to keep the analysis as simple as possible—but with the aim to put reliable bounds on our effective couplings—in this work we relate the mixing angle between light and heavy neutrinos ( $U_{eN}, U_{\mu N}, U_{\tau N}$ ) with the couplings as  $U \simeq \frac{\alpha_{\mathcal{O}}^{(i)} v^2}{2\Lambda^2}$ , where  $v$  corresponds to the vacuum expectation value:  $v = 250 \text{ GeV}$ .

As has been remarked in [7,8], the bounds for low sterile neutrino masses, coming from beam dump and rare LNV decays of mesons, are heavily dependent on the decay modes considered. As the effective lagrangian we are considering leads to the decay mode to a photon and an ordinary neutrino, those bounds do not apply in this work. For  $m_N$  in the range above a few hundred GeV, the electroweak precision data involving lepton number violating processes put the most stringent bounds on the neutrino mixings, except for the coupling constants of the first fermions family where the most stringent limits come from  $0\nu\beta\beta$ -decay. For the second and third families, we find that the most restrictive are the EWPD constraints. In the following we explain how these bounds are translated to the effective couplings  $\alpha_{\mathcal{O}}^i$ .

Some of the considered operators contribute directly to the neutrinoless double beta decay ( $0\nu\beta\beta$ -decay) and thus the corresponding coupling constants, involving the first fermion family  $i = 1$ , are restricted by strong bounds. We explicitly calculated the implications for the effective couplings in our lagrangian.

In a general way, the following effective interaction Hamiltonian can be considered:

$$\mathcal{H} = G_{\text{eff}} \bar{u} \Gamma d \quad \bar{e} \Gamma N + h.c. \tag{7}$$

where  $\Gamma$  represents a general Lorentz–Dirac structure. Following the development presented in [70] we find

$$G_{\text{eff}} \leq A \times 10^{-8} \left( \frac{m_N}{100 \text{ GeV}} \right)^{1/2} \text{ GeV}^{-2}$$

where the numerical constant  $A$  depends on the nuclear model used and the lifetime for the  $0\nu\beta\beta$ -decay. We take the most stringent limit  $\tau_{0\nu\beta\beta} \geq 1.1 \times 10^{26}$  years obtained by the KamLAND-Zen Collaboration [71].

In the effective theory we are considering the lowest order contribution to  $0\nu\beta\beta$ -decay comes from the operators containing the  $W$  field and the four-fermion operators with quarks  $u, d$ , the lepton  $e$ , and the Majorana neutrino  $N$ . These operators contribute to the effective Hamiltonian (7), with  $G_{\text{eff}} = \frac{\alpha}{\Lambda^2}$ , which, as we discussed in the paragraph after Eq. (6), is related with the mixing angle between light and heavy neutrinos as  $U_{iN}^2 = \left( \frac{\alpha v}{2\Lambda^2} \right)^2$ . We find that the value  $A = 3.2$  fits very well the bounds obtained for the mixings [7, 72] in the literature.

We can translate the limit coming from  $G_{\text{eff}}$  on  $\alpha_{\mathcal{O}}^{(1)}$ , which, for  $\Lambda = 1 \text{ TeV}$ , is

$$\alpha_{0\nu\beta\beta}^{\text{bound}} \leq 3.2 \times 10^{-2} \left( \frac{m_N}{100 \text{ GeV}} \right)^{1/2}. \tag{8}$$

On the other hand, to consider the existing bounds coming from collider, electroweak precision data (EWPD) and lepton-flavor-violating (LFV) processes we define, following [73]:  $\Omega_{ll'} = U_{lN}U_{l'N}$  where the allowed values for the parameters are [74]:

$$\Omega_{ee} \leq 0.0054, \quad \Omega_{\mu\mu} \leq 0.0096, \quad \Omega_{\tau\tau} \leq 0.016.$$

For the LFV process, e.g.  $\mu \rightarrow e\gamma$ ,  $\mu \rightarrow eee$  and  $\tau \rightarrow eee$ , which are induced by the quantum effects of the heavy neutrinos, we have several bounds [27, 67, 75, 76] but the most restrictive one comes from  $Br(\mu \rightarrow e\gamma) \leq 5.7 \cdot 10^{-13}$  [76, 77]. This bound imposes  $|\Omega_{e\mu}| \leq 0.0001$ , and can be translated to the constants  $\alpha$ ,

$$\Omega_{e\mu} = U_{eN}U_{\mu N} = \left( \frac{\alpha v^2}{2\Lambda^2} \right)^2 < 0.0001,$$

and for  $\Lambda = 1 \text{ TeV}$  we have

$$\alpha_{\text{EWPD}}^{\text{bound}} \leq 0.32. \tag{9}$$

In order to simplify the discussion, for the numerical evaluation we only consider the two following situations. In the set we call **A** the couplings associated to the operators that contribute to the  $0\nu\beta\beta$ -decay ( $\mathcal{O}_{Ne\phi}$ ,  $\mathcal{O}_{duNe}$ ,  $\mathcal{O}_{QuNL}$ ,  $\mathcal{O}_{LNQd}$ , and  $\mathcal{O}_{QNld}$ ) for the first family are restricted to the corresponding bound  $\alpha_{0\nu\beta\beta}^{\text{bound}}$  and the other constants are

restricted to the bound determined by EWPD  $\alpha_{\text{EWPD}}^{\text{bound}}$ . In the case of the set called **B** all the couplings are restricted to the  $0\nu\beta\beta$  bound  $\alpha_{0\nu\beta\beta}^{\text{bound}}$ , which is the most stringent. For the 1-loop generated operators we consider the coupling constant as  $1/(16\pi^2)$  times the corresponding tree-level coupling:  $\alpha^{1\text{-loop}} = \alpha^{\text{tree}}/(16\pi^2)$ . Thus, for the operators  $\mathcal{O}_{DN}$ ,  $\mathcal{O}_{NW}$  and  $\mathcal{O}_{\bar{D}N}$ , which contribute to  $0\nu\beta\beta$ , we have

$$\alpha_{L_2}^{(1)}, \alpha_{L_3}^{(1)}, \alpha_{L_4}^{(1)} \sim \frac{1}{16\pi^2} \alpha_{0\nu\beta\beta}^{\text{bound}}$$

for fermions of the first family. For the remaining operators we take

$$\alpha \sim \alpha_{\text{EWPD}}^{\text{bound}}, \alpha_{0\nu\beta\beta}^{\text{bound}}$$

in the sets **A** and **B**, respectively.

### 4 Final remarks

Searches for heavy neutrinos often rely on the possibility that they may decay to detectable particles. The interpretation of the corresponding results of such searches requires a model for the heavy neutrino decay. In this work we consider an effective approach for heavy Majorana neutrino interactions, and we calculate the branching ratios for the different decay modes.

Depending on the Majorana neutrinos mass scale, the decay can have effects on different physical contexts like solar/astrophysical neutrinos, collider searches like the those taking place at the LHC, neutrino experiments as OPERA, MiniBoone, SHALON, etc. In particular, the effects on some of this experiments for low mass neutrinos were discussed in [58].

Summarizing, we calculated the decay modes for the Majorana neutrinos  $N$  in an effective theory approach. We presented the analytical results for the dominant channels, discussed the existent bounds taken into account for the effective couplings, and displayed the different branching ratios and the total decay width for the heavy sterile neutrino considered.

**Acknowledgments** We thank CONICET (Argentina) and Universidad Nacional de Mar del Plata (Argentina); and PEDECIBA, ANII, and CSIC-UdelaR (Uruguay) for their financial supports.

**Open Access** This article is distributed under the terms of the Creative Commons Attribution 4.0 International License (<http://creativecommons.org/licenses/by/4.0/>), which permits unrestricted use, distribution, and reproduction in any medium, provided you give appropriate credit to the original author(s) and the source, provide a link to the Creative Commons license, and indicate if changes were made. Funded by SCOAP<sup>3</sup>.

**Appendix A: Complete effective lagrangian**

We present here the complete effective lagrangian obtained from the operators listed in (2), (3) and (4). The full contributions are considered for the total Majorana neutrino decay width  $\Gamma_N$ ,

$$\begin{aligned} \mathcal{L}_{SVB}^{\text{tree}} = & \frac{1}{\Lambda^2} \left\{ \alpha_{\phi}^{(i)} \left( \frac{3v^2}{2\sqrt{2}} \bar{\nu}_{L,i} N_R h + \frac{3v}{2\sqrt{2}} \bar{\nu}_{L,i} N_R hh \right. \right. \\ & \left. \left. + \frac{1}{2\sqrt{2}} \bar{\nu}_{L,i} N_R hhh \right) \right. \\ & - \alpha_Z \left( -(\bar{N}_R \gamma^\mu N_R) \left( \frac{m_Z}{v} Z_\mu \right) \left( \frac{v^2}{2} + vh + \frac{1}{2} hh \right) \right. \\ & \left. + (\bar{N}_R \gamma^\mu N_R) \left( \frac{v}{2} P_\mu^{(h)} h + \frac{1}{2} P_\mu^{(h)} hh \right) \right) \\ & - \alpha_W^{(i)} (\bar{N}_R \gamma^\mu l_R) \left( \frac{vm_W}{\sqrt{2}} W_\mu^+ + \sqrt{2} m_W W_\mu^+ h \right. \\ & \left. + \frac{g}{2\sqrt{2}} W_\mu^+ hh \right) + h.c. \left. \right\}. \end{aligned} \tag{A1}$$

In (A1) a sum over the family index  $i$  is understood, and the constants  $\alpha_{\mathcal{O}}^{(i)}$  are associated to the specific operators:

$$\alpha_Z = \alpha_{NN\phi}, \alpha_{\phi}^{(i)} = \alpha_{LN\phi}^{(i)}, \alpha_W^{(i)} = \alpha_{Ne\phi}^{(i)}.$$

The four-fermion contact operators presented in (3) lead to the tree-level lagrangian:

$$\begin{aligned} \mathcal{L}_{4-f}^{\text{tree}} = & \frac{1}{\Lambda^2} \left\{ \alpha_{V_0}^{(i)} \bar{d}_{R,i} \gamma^\mu u_{R,i} \bar{N}_R \gamma_\mu l_{R,i} + \alpha_{V_1}^{(i)} \bar{l}_{R,i} \gamma^\mu l_{R,i} \bar{N}_R \gamma_\mu N_R \right. \\ & + \alpha_{V_2}^{(i)} \bar{L}_i \gamma^\mu L_i \bar{N}_R \gamma_\mu N_R \\ & + \alpha_{V_3}^{(i)} \bar{u}_{R,i} \gamma^\mu u_{R,i} \bar{N}_R \gamma_\mu N_R + \alpha_{V_4}^{(i)} \bar{d}_{R,i} \gamma^\mu d_{R,i} \bar{N}_R \gamma_\mu N_R \\ & + \alpha_{V_5}^{(i)} \bar{Q}_i \gamma^\mu Q_i \bar{N}_R \gamma_\mu N_R \\ & + \alpha_{S_0}^{(i)} (\bar{\nu}_{L,i} N_R \bar{e}_{L,i} l_{R,i} - \bar{e}_{L,i} N_R \bar{\nu}_{L,i} l_{R,i}) \\ & + \alpha_{S_1}^{(i)} (\bar{u}_{L,i} u_{R,i} \bar{N}_R \nu_{L,i} + \bar{d}_{L,i} u_{R,i} \bar{N}_R e_{L,i}) \\ & + \alpha_{S_2}^{(i)} (\bar{\nu}_{L,i} N_R \bar{d}_{L,i} d_{R,i} - \bar{e}_{L,i} N_R \bar{u}_{L,i} d_{R,i}) \\ & + \alpha_{S_3}^{(i)} (\bar{u}_{L,i} N_R \bar{e}_{L,i} d_{R,i} - \bar{d}_{L,i} N_R \bar{\nu}_{L,i} d_{R,i}) \\ & \left. + \alpha_{S_4}^{(i)} (\bar{N}_R \nu_{L,i} \bar{l}_{L,i} N_R + \bar{N}_R e_{L,i} \bar{e}_{L,i} N_R) + h.c. \right\}. \end{aligned} \tag{A2}$$

In (A2) a sum over the family index  $i$  is understood, and the constants  $\alpha_{\mathcal{O}}^{(i)}$  are associated to the specific operators:

$$\begin{aligned} \alpha_{V_0}^{(i)} &= \alpha_{duNe}^{(i)}, \alpha_{V_1}^{(i)} = \alpha_{eNN}^{(i)}, \alpha_{V_2}^{(i)} = \alpha_{LNN}^{(i)}, \\ \alpha_{V_3}^{(i)} &= \alpha_{uNN}^{(i)}, \alpha_{V_4}^{(i)} = \alpha_{dNN}^{(i)}, \alpha_{V_5}^{(i)} = \alpha_{QNN}^{(i)}, \\ \alpha_{S_0}^{(i)} &= \alpha_{LNe}^{(i)}, \alpha_{S_1}^{(i)} = \alpha_{QuNL}^{(i)}, \alpha_{S_2}^{(i)} = \alpha_{LNQd}^{(i)}, \\ \alpha_{S_3}^{(i)} &= \alpha_{QNLd}^{(i)}, \alpha_{S_4}^{(i)} = \alpha_{LN}^{(i)}. \end{aligned}$$

The one-loop level generated operators in (4) give the lagrangian:

$$\begin{aligned} \mathcal{L}_{\text{eff}}^{1\text{-loop}} = & \frac{\alpha_{L_1}^{(i)}}{\Lambda^2} \left( -i\sqrt{2} v c_W P_\mu^{(A)} \bar{\nu}_{L,i} \sigma^{\mu\nu} N_R A_\nu \right. \\ & + i\sqrt{2} v s_W P_\mu^{(Z)} \bar{\nu}_{L,i} \sigma^{\mu\nu} N_R Z_\nu + \\ & - i\sqrt{2} c_W P_\mu^{(A)} \bar{\nu}_{L,i} \sigma^{\mu\nu} N_R A_\nu h \\ & \left. + i\sqrt{2} s_W P_\mu^{(Z)} \bar{\nu}_{L,i} \sigma^{\mu\nu} N_R Z_\nu h \right) \\ & - \frac{\alpha_{L_2}^{(i)}}{\Lambda^2} \left( \frac{m_Z}{\sqrt{2}} P_\mu^{(N)} \bar{\nu}_{L,i} N_R Z^\mu + \frac{m_z}{\sqrt{2}v} P_\mu^{(N)} \bar{\nu}_{L,i} N_R Z^\mu h \right. \\ & + m_W P_\mu^{(N)} \bar{l}_{L,i} N_R W^{-\mu} + \frac{\sqrt{2} m_W}{v} P_\mu^{(N)} \bar{l}_{L,i} N_R W^{-\mu} h \\ & \left. + \frac{1}{\sqrt{2}} P_\mu^{(h)} P^{(N)\mu} \bar{\nu}_{L,i} N_R h \right) \\ & - \frac{\alpha_{L_3}^{(i)}}{\Lambda^2} \left( i\sqrt{2} v c_W P_\mu^{(Z)} \bar{\nu}_{L,i} \sigma^{\mu\nu} N_R Z_\nu \right. \\ & + i\sqrt{2} v s_W P_\mu^{(A)} \bar{\nu}_{L,i} \sigma^{\mu\nu} N_R A_\nu \\ & + i2\sqrt{2} m_W \bar{\nu}_{L,i} \sigma^{\mu\nu} N_R W_\mu^+ W_\nu^- \\ & + i\sqrt{2} v P_\mu^{(W)} \bar{l}_{L,i} \sigma^{\mu\nu} N_R W_\nu^- \\ & + i4m_W c_W \bar{l}_{L,i} \sigma^{\mu\nu} N_R W_\mu^- Z_\nu \\ & + i4m_W s_W \bar{l}_{L,i} \sigma^{\mu\nu} N_R W_\mu^- A_\nu \\ & + i\sqrt{2} P_\mu^{(W)} \bar{l}_{L,i} \sigma^{\mu\nu} N_R W_\nu^- h \\ & + i2g c_W \bar{l}_{L,i} \sigma^{\mu\nu} N_R W_\nu^- Z_\mu h \\ & + i2g s_W \bar{l}_{L,i} \sigma^{\mu\nu} N_R W_\nu^- A_\mu h \\ & + i\sqrt{2} c_W P_\mu^{(Z)} \bar{\nu}_{L,i} \sigma^{\mu\nu} N_R Z_\mu h \\ & + i\sqrt{2} s_W P_\mu^{(A)} \bar{\nu}_{L,i} \sigma^{\mu\nu} N_R A_\mu h \\ & \left. + i\sqrt{2} g \bar{\nu}_{L,i} \sigma^{\mu\nu} N_R W_\mu^+ W_\nu^- h \right) \\ & - \frac{\alpha_{L_4}^{(i)}}{\Lambda^2} \left( \frac{m_Z}{\sqrt{2}} P_\mu^{(\bar{\nu})} \bar{\nu}_{L,i} N_R Z_\mu \right. \\ & + \frac{m_Z}{\sqrt{2}v} (P_\mu^{(\bar{\nu})} - P_\mu^{(h)}) \bar{\nu}_{L,i} N_R Z^\mu h \\ & + \frac{1}{\sqrt{2}} P^{(h)\mu} P_\mu^{(\bar{\nu})} \bar{\nu}_{L,i} N_R h \\ & - \frac{\sqrt{2} m_W^2}{v} \bar{\nu}_{L,i} N_R W^{-\mu} W_\mu^+ - \frac{m_z^2}{\sqrt{2}v} \bar{\nu}_{L,i} N_R Z_\mu Z^\mu \\ & - \frac{1}{2} \frac{m_Z^2}{v^2} \bar{\nu}_{L,i} N_R Z_\mu Z^\mu h \\ & - \frac{\sqrt{2} m_W^2}{v^2} \bar{\nu}_{L,i} N_R W_\mu^+ W^{-\mu} h \\ & + m_W P_\mu^{(\bar{l})} W^{-\mu} \bar{l}_{L,i} N_R \\ & + \frac{m_W}{v} (P_\mu^{(\bar{l})} - P_\mu^{(h)}) W^{-\mu} \bar{l}_{L,i} N_R h \\ & + em_W \bar{l}_{L,i} N_R W^{-\mu} A_\mu + em_Z s_W \bar{l}_{L,i} N_R W^{-\mu} Z_\mu \\ & + \frac{em_Z s_W}{v} \bar{l}_{L,i} N_R Z_\mu W^{-\mu} h \\ & \left. + \frac{em_Z c_W}{\sqrt{2}v} \bar{l}_{L,i} N_R A_\mu W^{-\mu} h \right) + h.c. \end{aligned} \tag{A3}$$



where  $P^{(a)}$  is the 4-moment of the incoming  $a$ -particle and a sum over the family index  $i$  is understood again. The constants  $\alpha_{L_j}^{(i)}$  with  $j = 1, 2, 3, 4$  are associated to the specific operators:

$$\alpha_{L_1}^{(i)} = \alpha_{NB}^{(i)}, \quad \alpha_{L_2}^{(i)} = \alpha_{DN}^{(i)}, \quad \alpha_{L_3}^{(i)} = \alpha_{NW}^{(i)}, \quad \alpha_{L_4}^{(i)} = \alpha_{\bar{D}N}^{(i)}.$$

### Appendix B: Fermionic three-body decay widths

For the decays to one lepton and two quarks we have the expressions

$$\begin{aligned} \frac{d\Gamma^{(N \rightarrow l^+ \bar{u} d)}}{dx} &= \frac{m_N}{512\pi^3} \left(\frac{m_N}{\Lambda}\right)^4 x \frac{(1-x-y_l+y_u)}{(1-x+y_l)^3} \\ &\times \left\{ (1-x+y_l-y_u) \left[ 6\alpha_1^{i_u, i_l} x(1-x+y_l)^2 \right. \right. \\ &+ 12\alpha_2^{i_u, i_l} (2-x)(1-x+y_l)\sqrt{y_l y_u} \\ &+ \alpha_3^{i_u, i_l} (2x^3 - x^2(5+5y_l+y_u) - 4y_l(1+y_l+2y_u) \\ &+ x(3+10y_l+3y_l^2+3y_u+3y_l y_u)) \left. \right] \\ &+ 24\alpha_4^{i_u, i_l} x(1-x+y_l)^2\sqrt{y_l y_u} \left. \right\} \end{aligned} \tag{B1}$$

with  $2\sqrt{y_l} < x < 1+y_l-y_u$ ,  $y_l = m_l^2/m_N^2$ ,  $y_u = m_u^2/m_N^2$ , and for the coefficients  $\alpha_{1,\dots,4}$

$$\begin{aligned} \alpha_1^{i_u, i_l} &= \left( \alpha_{s_1}^{(i_u)^2} + \alpha_{s_2}^{(i_u)^2} - \alpha_{s_2}^{(i_u)} \alpha_{s_3}^{(i_u)} \right) \delta^{i_u, i_l} \\ \alpha_2^{i_u, i_l} &= \left( \alpha_{s_1}^{(i_u)} \alpha_W^{(i_l)} \frac{y_W(1-x+y_l-y_W)}{(1-x+y_l-y_W)^2 + y_W y_{\Gamma W}} \right. \\ &\quad \left. - \alpha_{s_3}^{(i_u)} \alpha_{V_0}^{(i_u)} \right) \delta^{i_u, i_l} \\ \alpha_3^{i_u, i_l} &= \left( \alpha_{s_3}^{(i_u)^2} + 4\alpha_{V_0}^{(i_u)^2} \right) \delta^{i_u, i_l} \\ &\quad + 4\alpha_W^{(i_l)^2} \frac{y_W^2(1-x+y_l-y_W)}{(1-x+y_l-y_W)^2 + y_W y_{\Gamma W}} \\ \alpha_4^{i_u, i_l} &= \alpha_{s_2}^{(i_u)} \alpha_{V_0}^{(i_u)} \delta^{i_u, i_l}, \end{aligned}$$

$$\begin{aligned} \frac{d\Gamma^{(N \rightarrow \nu d d)}}{dx} &= \frac{m_N}{128\pi^3} \left(\frac{m_N}{\Lambda}\right)^4 \frac{x^2 ((1-x)(1-x-4y_d))^{1/2}}{4(1-x)^2} \\ &\times \left\{ \delta^{i_l, i_d} \alpha_{s_3}^{(i_l)^2} (3+x(-5+2x+2y_d)) \right. \\ &+ 6 \left( \tilde{\alpha}_1^{i_l, i_d} + \tilde{\alpha}_2^{i_l, i_d} - \delta^{i_l, i_d} \tilde{\alpha}_3^{i_l, i_d} \alpha_{s_3}^{i_l} \right) \\ &\times (1-x)(1-x-2y_d) \left. \right\} \end{aligned}$$

with  $0 < x < 1-4y_d$ ,  $y_d = m_d^2/m_N^2$ , and

$$\begin{aligned} \tilde{\alpha}_1^{i_l, i_d} &= \left( \delta^{i_l, i_d} \alpha_{s_2}^{(i_l)} + \alpha_{\phi}^{(i_l)} c \frac{(1-x-y_h)}{D} \right)^2 \\ &+ \alpha_{\phi}^{(i_l)^2} c^2 \frac{y_h y_{\Gamma h}}{D_h^2}, \end{aligned}$$

$$\begin{aligned} \tilde{\alpha}_2^{i_l, i_d} &= \alpha_{\phi}^{(i_l)} \frac{c^2}{D_h} \\ \tilde{\alpha}_3^{i_l, i_d} &= \delta^{i_l, i_d} \alpha_{s_2}^{(i_l)} + \alpha_{\phi}^{(i_l)} c \frac{(1-x-y_h)}{D_h}, \\ y_h &= m_h^2/m_N^2, \quad y_{\Gamma h} = \Gamma_h^2/m_N^2, \\ D_h &= (1-x-y_h)^2 + y_h y_{\Gamma h}, \quad c = \frac{3gv^2 m_d}{4\sqrt{2}m_N^2 m_W}, \end{aligned}$$

$$\begin{aligned} \frac{d\Gamma^{(N \rightarrow \nu u u)}}{dx} &= \frac{m_N}{128\pi^3} \left(\frac{m_N}{\Lambda}\right)^4 \tilde{\alpha}^{i_l, i_u} \frac{3}{2} x^2 \left(1 - \frac{4y_u}{(1-x)}\right)^{1/2} \\ &\times (1-x-2y_u) \delta_{i_u, i_l} \end{aligned}$$

with  $0 < x < 1-4y_u$  and

$$\tilde{\alpha}^{i_l, i_u} = \delta^{i_l, i_u} \alpha_{s_1}^{(i_l)^2} + 2\alpha_{\phi}^{(i_l)^2} \frac{c^2}{D_h}, \quad c = \frac{3gv^2 m_u}{4\sqrt{2}m_N^2 m_W}.$$

The purely leptonic decay gives

$$\begin{aligned} \frac{d\Gamma^{(N \rightarrow l^+ leptons)}}{dx} &= \frac{m_N}{1536\pi^3} \left(\frac{m_N}{\Lambda}\right)^4 \frac{(1-x+y_l-y_{l'})^2}{(1-x+y_l)^3} \\ &\times x \left[ \alpha_1^{i_l, i_{l'}} P(x) - \alpha_2^{i_l, i_{l'}} R(x) \right] \end{aligned}$$

with  $2\sqrt{y_l} < x < 1+y_l-y_{l'}$ ,  $y_l = m_l^2/m_N^2$ ,  $y_{l'} = m_{l'}^2/m_N^2$ , and  $\alpha_{1,2}$ ; and for the terms  $P(x)$ ,  $R(x)$  we have

$$\begin{aligned} \alpha_1^{i_l, i_{l'}} &= \alpha_{s_0}^{(i_l)^2} \delta^{i_l, i_{l'}} + \frac{4\alpha_W^{(i_l)^2} y_W^2}{(1-x+y_l-y_W)^2 + y_W y_{\Gamma W}} \\ \alpha_2^{i_l, i_{l'}} &= 12\alpha_{s_0}^{(i_{l'})} \alpha_W^{(i_l)} \frac{(1-x+y_l-y_W)}{(1-x+y_l-y_W)^2 + y_W y_{\Gamma W}} \delta^{i_l, i_{l'}}, \\ P(x) &= 2x^3 - x^2(5+5y_l+y_{l'}) - 4y_l(1+y_l+2y_{l'}) \\ &\quad + x(3+10y_l+3y_{l'}^2+3y_{l'}+3y_l y_{l'}), \\ R(x) &= (2-x)(1-x+y_l)(y_l y_{l'})^{1/2}. \end{aligned}$$

### References

1. P. Minkowski, Phys. Lett. B **67**, 421 (1977)
2. R.N. Mohapatra, G. Senjanovic, Phys. Rev. Lett. **44**, 912 (1980)
3. T. Yanagida, Prog. Theor. Phys. **64**, 1103 (1980)
4. M. Gell-Mann, P. Ramond, R. Slansky, Conf. Proc. C **790927**, 315 (1979). [arXiv:1306.4669](https://arxiv.org/abs/1306.4669)
5. J. Schechter, J.W.F. Valle, Phys. Rev. D **22**, 2227 (1980)
6. B. Kayser, F. Gibrat-Debu, F. Perrier, World Sci. Lect. Notes Phys. **25**, 1 (1989)
7. A. de Gouvêa and A. Kobach, Phys. Rev. D **93**, 033005 (2016). [arXiv:1511.00683](https://arxiv.org/abs/1511.00683)
8. F.F. Deppisch, P.S. Bhupal Dev, A. Pilaftsis, N. J. Phys. **17**, 075019 (2015). [arXiv:1502.06541](https://arxiv.org/abs/1502.06541)
9. F. del Aguila, S. Bar-Shalom, A. Soni, J. Wudka, Phys. Lett. B **670**, 399 (2009). [arXiv:0806.0876](https://arxiv.org/abs/0806.0876)
10. E. Ma, J.T. Pantaleone, Phys. Rev. D **40**, 2172 (1989)
11. W. Buchmuller, C. Greub, Nucl. Phys. B **363**, 345 (1991)
12. A. Hofer, L. Sehgal, Phys. Rev. D **54**, 1944 (1996). [arXiv:hep-ph/9603240](https://arxiv.org/abs/hep-ph/9603240)

13. J. Peressutti, I. Romero, O.A. Sampayo, Phys. Rev. D **84**, 113002 (2011). [arXiv:1110.0959](#)
14. C. Blaksley, M. Blennow, F. Bonnet, P. Coloma, E. Fernandez-Martinez, Nucl. Phys. B **852**, 353 (2011). [arXiv:1105.0308](#)
15. L. Duarte, G.A. González-Sprinberg, O.A. Sampayo, Phys. Rev. D **91**, 053007 (2015). [arXiv:1412.1433](#)
16. S. Antusch, O. Fischer, JHEP **05**, 053 (2015). [arXiv:1502.05915](#)
17. S. Banerjee, P.S.B. Dev, A. Ibarra, T. Mandal, M. Mitra, Phys. Rev. D **92**, 075002 (2015). [arXiv:1503.05491](#)
18. S. Bray, J.S. Lee, A. Pilaftsis, Phys. Lett. B **628**, 250 (2005). [arXiv:hep-ph/0508077](#)
19. J. Peressutti, O. Sampayo, J.I. Aranda, Phys. Rev. D **64**, 073007 (2001). [arXiv:hep-ph/0105162](#)
20. J. Peressutti, O. Sampayo, Phys. Rev. D **67**, 017302 (2003). [arXiv:hep-ph/0211355](#)
21. W.-Y. Keung, G. Senjanovic, Phys. Rev. Lett. **50**, 1427 (1983)
22. A. Datta, M. Guchait, A. Pilaftsis, Phys. Rev. D **50**, 3195 (1994). [arXiv:hep-ph/9311257](#)
23. J. Almeida, F.M.L., Y.D.A. Coutinho, J.A. Martins Simoes, M. do Vale, Phys. Rev. D **62**, 075004 (2000). [arXiv:hep-ph/0002024](#)
24. A. Atre, T. Han, S. Pascoli, B. Zhang, JHEP **0905**, 030 (2009). [arXiv:0901.3589](#)
25. F. del Aguila, J.A. Aguilar-Saavedra, R. Pittau, JHEP **10**, 047 (2007). [arXiv:hep-ph/0703261](#)
26. S. Kovalenko, Z. Lu, I. Schmidt, Phys. Rev. D **80**, 073014 (2009). [arXiv:0907.2533](#)
27. D. Alva, T. Han, R. Ruiz, JHEP **02**, 072 (2015). [arXiv:1411.7305](#)
28. A. Das, N. Okada, Phys. Rev. D **93**, 033003 (2016). [arXiv:1510.04790](#)
29. C.O. Dib, C.S. Kim, Phys. Rev. D **92**, 093009 (2015). [arXiv:1509.05981](#)
30. E. Izaguirre, B. Shuve, Phys. Rev. D **91**, 093010 (2015). [arXiv:1504.02470](#)
31. A. Das, P. Konar, S. Majhi (2016). [arXiv:1604.00608](#)
32. C. Degrande, O. Mattelaer, R. Ruiz, J. Turner (2016). [arXiv:1602.06957](#)
33. P.S.B. Dev, A. Pilaftsis, U.K. Yang, Phys. Rev. Lett. **112**, 081801 (2014). [arXiv:1308.2209](#)
34. V. Khachatryan et al. (CMS), Phys. Lett. B **748**, 144 (2015). [arXiv:1501.05566](#)
35. G. Aad et al. (ATLAS), JHEP **07**, 162 (2015). [arXiv:1506.06020](#)
36. G. Aad et al. (ATLAS Collaboration), JHEP **1110**, 107 (2011). [arXiv:1108.0366](#)
37. G. Aad et al. (ATLAS Collaboration), Eur. Phys. J. C **72**, 2056 (2012). [arXiv:1203.5420](#)
38. R.N. Mohapatra, Phys. Rev. Lett. **56**, 561 (1986)
39. R.N. Mohapatra, J.W.F. Valle, Phys. Rev. D **34**, 1642 (1986)
40. J. Bernabeu, A. Santamaria, J. Vidal, A. Mendez, J.W.F. Valle, Phys. Lett. B **187**, 303 (1987)
41. E. Arganda, M.J. Herrero, X. Marcano, C. Weiland, Phys. Lett. B **752**, 46 (2016). [arXiv:1508.05074](#)
42. A. Das, N. Okada, Phys. Rev. D **88**, 113001 (2013). [arXiv:1207.3734](#)
43. A. Das, P.S. Bhupal Dev, N. Okada, Phys. Lett. B **735**, 364 (2014). [arXiv:1405.0177](#)
44. J. Gluza, T. Jelinski, R. Szafron (2016). [arXiv:1604.01388](#)
45. G. Aad et al. (ATLAS), Phys. Rev. D **88**, 012001 (2013). [arXiv:1304.6310](#)
46. J.C. Helo, M. Hirsch, S. Kovalenko, Phys. Rev. D **89**, 073005 (2014). [arXiv:1312.2900](#)
47. G. Aad et al. (ATLAS), Phys. Rev. D **92**, 072004 (2015). [arXiv:1504.05162](#)
48. G. Aad et al. (ATLAS), Phys. Rev. D **91**, 012008 (2015). [arXiv:1411.1559](#). [Erratum: Phys. Rev. D **92**, no. 5, 059903 (2015)]
49. A.M. Gago, P. Hernandez, J. Jones-Pérez, M. Losada, A.M. Briceo, Eur. Phys. J. C **75**, 470 (2015). [arXiv:1505.05880](#)
50. S. Biswas, J. Chakraborty, S. Roy, Phys. Rev. D **83**, 075009 (2011). [arXiv:1010.0949](#)
51. S. Antusch, E. Cazzato, O. Fischer (2016). [arXiv:1604.02420](#)
52. B. Batell, M. Pospelov, B. Shuve (2016). [arXiv:1604.06099](#)
53. G. Pagliaroli, A. Palladino, F. L. Villante, F. Vissani, Phys. Rev. D **92**, 113008 (2015). [arXiv:1506.02624](#)
54. M. Masip, P. Masjuan, Phys. Rev. D **83**, 091301 (2011). [arXiv:1103.0689](#)
55. M. Ross-Lonergan, J. Phys. Conf. Ser. **598**, 012028 (2015)
56. M. Masip, P. Masjuan, D. Meloni, JHEP **01**, 106 (2013). [arXiv:1210.1519](#)
57. C. Dib, J. C. Helo, M. Hirsch, S. Kovalenko, I. Schmidt, Phys. Rev. D **85**, 011301 (2012). [arXiv:1110.5400](#)
58. L. Duarte, J. Peressutti, O.A. Sampayo, Phys. Rev. D **92**, 093002 (2015). [arXiv:1508.01588](#)
59. G.L. Fogli, E. Lisi, A. Mirizzi, D. Montanino, Nucl. Phys. Proc. Suppl. **143**, 505 (2005)
60. S.-H. Kim, K.-I. Takemasa, Y. Takeuchi, S. Matsuura, J. Phys. Soc. Jpn. **81**, 024101 (2012). [arXiv:1112.4568](#)
61. J. Wudka, AIP Conf. Proc. **531**, 81 (2000). [arXiv:hep-ph/0002180](#)
62. J. Wudka, AIP Conf. Proc. **1116**, 247 (2009)
63. C. Arzt, M. Einhorn, J. Wudka, Nucl. Phys. B **433**, 41 (1995). [arXiv:hep-ph/9405214](#)
64. R. Kleiss, W.J. Stirling, S. Ellis, Comput. Phys. Commun. **40**, 359 (1986)
65. A.A. Aguilar-Arevalo et al. (MiniBooNE), Phys. Rev. Lett. **102**, 101802 (2009). [arXiv:0812.2243](#)
66. V.G. SinitSYna, M. Masip, V.Y. SinitSYna, EPJ Web Conf. **52**, 09010 (2013)
67. M. Drewes, B. Garbrecht (2015). [arXiv:1502.00477](#)
68. F. del Aguila, J.A. Aguilar-Saavedra, R. Pittau, J. Phys. Conf. Ser. **53**, 506 (2006). [arXiv:hep-ph/0606198](#)
69. F. del Aguila et al., Eur. Phys. J. C **57**, 183 (2008). [arXiv:0801.1800](#)
70. R. Mohapatra, Nucl. Phys. Proc. Suppl. **77**, 376 (1999). [arXiv:hep-ph/9808284](#)
71. A. Gando et al. (KamLAND-Zen) (2016). [arXiv:1605.02889](#)
72. A. Faessler, M. González, S. Kovalenko, F. Šimkovic, Phys. Rev. D **90**, 096010 (2014). [arXiv:1408.6077](#)
73. F. del Aguila, J. Aguilar-Saavedra, JHEP **0505**, 026 (2005). [arXiv:hep-ph/0503026](#)
74. S. Bergmann, A. Kagan, Nucl. Phys. B **538**, 368 (1999). [arXiv:hep-ph/9803305](#)
75. S. Antusch, O. Fischer, JHEP **10**, 94 (2014). [arXiv:1407.6607](#)
76. D. Tommasini, G. Barenboim, J. Bernabeu, C. Jarlskog, Nucl. Phys. B **444**, 451 (1995). [arXiv:hep-ph/9503228](#)
77. F. del Aguila, J. de Blas, M. Perez-Victoria, Phys. Rev. D **78**, 013010 (2008). [arXiv:0803.4008](#)